October 15, 2010

Dipole Source Encoding and Tracking by the Goldfish Auditory System

Sheryl L. Coombs, *Bowling Green State University*
Richard R. Fay
Andreas Elepfandt

The Journal of Experimental Biology 213, 3536-3547

doi:10.1242/jeb.044909

Dipole source encoding and tracking by the goldfish auditory system

Sheryl Coombs[1,*], Richard R. Fay[2] and Andreas Elepfandt[3]

[1]Department of Biological Sciences and JP Scott Center for Neuroscience, Mind and Behavior, Bowling Green State University, Bowling Green, OH 43403, USA, [2]Parmly Hearing Institute and Department of Psychology, Loyola University Chicago, Chicago, IL 60626, USA and [3]Institute of Biology, Humboldt University Berlin, E-10015 Berlin, Germany

*Author for correspondence (scoombs@bgsu.edu)

Accepted 25 July 2010

SUMMARY

In goldfish and other otophysans, the Weberian ossicles mechanically link the saccule of the inner ear to the anterior swimbladder chamber (ASB). These structures are correlated with enhanced sound-pressure sensitivity and greater sensitivity at high frequencies (600–2000 Hz). However, surprisingly little is known about the potential impact of the ASB on other otolithic organs and about how auditory responses are modulated by discrete sources that change their location or orientation with respect to the ASB. In this study, saccular and lagenar nerve fiber responses and conditioned behaviors of goldfish were measured to a small, low-frequency (50 Hz) vibrating sphere (dipole) source as a function of its location along the body and its orientation with respect to the ASB. Conditioned behaviors and saccular nerve fiber activity exhibited response characteristics nearly identical to those measured from a hydrophone in the same relative position as the ASB. By contrast, response patterns from lagena fibers could not be predicted by pressure inputs to the ASB. Deflation of the ASB abolished the characteristic spatial response pattern of saccular but not lagena fibers. These results show that: (1) the lagena is not driven by ASB-mediated pressure inputs to the ear; (2) the ASB–saccule pathway dominates behavioral responsiveness, operating effectively at frequencies as low as 50 Hz; and (3) behavioral and neural (saccular) responses are strongly modulated by the position and orientation of the dipole with respect to the ASB.

Key words: saccule, lagena, primary afferents, swimbladder, conditioned behavior, Weberian ossicles.

INTRODUCTION

Although there is much information on the ability of goldfish to detect and process 100–2000 Hz sounds from a stationary monopole (loudspeaker) source (e.g. Fay, 1998a; Fay, 1998b; Fay, 2000), most natural sound sources are small, moving or vibrating bodies, i.e. dipoles, such as swimming fish (Kalmijn, 1988; Kalmijn, 1989). Sound fields associated with dipoles are axisymmetric, meaning that the spatial distribution of the pressure and particle velocity fields are complexly shaped, with a pressure maximum and particle motion minimum on the axis of movement or oscillation (Fig. 1). These dipole fields can exhibit large spatial differences in both pressure and particle motion (Sand, 1981; Kalmijn, 1988; Coombs et al., 1996).

Neurophysiological, computational modeling (Coombs et al., 1996) and behavioral studies (Coombs, 1994; Daily and Braun, 2009; Nauroth and Mogdans, 2009) indicate that small (~0.6–1.0 cm in diameter), nearby (less than one fish body length away), low frequency (<~200 Hz) dipole sources stimulate both the auditory and lateral line system of goldfish, but in systematically different ways. For lateral line nerve fibers innervating canal neuromasts, the relevant sensor is an individual neuromast, which responds proportionately to the pressure difference between adjacent canal pores (the pressure gradient) (Coombs et al., 1996). For auditory (saccular) nerve fibers, the relevant sensor is thought to be the anterior chamber of the swimbladder (ASB), which is mechanically coupled to the fluids of the saccular chamber by a series of modified vertebrae, the Weberian ossicles (Evans, 1925; von Frisch, 1938). Thus, the ASB behaves as a remote, sound-pressure transducer and amplifier: the gas-filled bladder expands and contracts in response to surrounding pressure changes and the motions of the swimbladder walls are transmitted to the inner ear fluids via the Weberian ossicles.

Given that all otolith organs of the inner ear behave as accelerometers (de Vries, 1950) that detect linear accelerations of the fish's body, it is possible that the goldfish lagena could be stimulated directly via the motion of the surrounding water and/or indirectly via re-radiated motions of the swimbladder. Although the ASB–Weberian ossicular chain is anatomically linked to the saccule and not the lagena, the lagena could nevertheless be stimulated by swimbladder motions transmitted through the intervening tissues. Indeed, some pressure-sensitive species (e.g. damselfish and cod) are known to respond to swimbladder-transmitted vibrations in this way without the benefit of any special connections between the ear and swimbladder (Chapman and Hawkins, 1973; Myrberg and Spires, 1980). However, there is no evidence so far that the lagena plays a role in sound detection.

In this study, we use neurophysiological techniques to characterize the response patterns of the goldfish inner ear (saccular and lagenar fibers) to a small, nearby dipole source that slowly changed its location along the length of the fish with respect to the ASB, and under conditions in which the ASB was inflated or deflated. When a small dipole source moves past a small pressure-sensitive sensor (hydrophone), it causes rather dramatic changes in pressure amplitude over very short travel distances (mm) (Coombs et al., 1996). Similarly, the direction and magnitude of particle motion also change as a function of source position (Sand, 1981; Denton and Gray, 1982). This is due to the spatial complexity of the stimulus field surrounding the dipole (Fig. 1). The response of directionally sensitive hair cells (particle motion sensors of the inner ear) will thus depend not only on the magnitude of particle motion, but also on its direction (or axis of motion) with respect to the orientation of the hair cells. Small dipole sources are thus ideal for characterizing

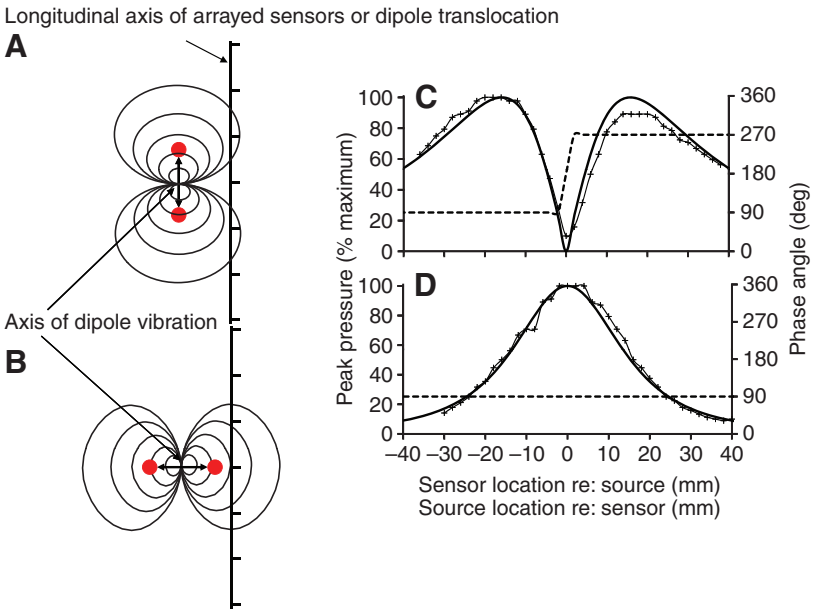

Fig. 1. Iso-pressure contours around two dipole sources: one that has an axis of vibration that is parallel to an array of pressure sensors (A) and one that is oriented perpendicular to the array (B). The computed (from dipole field equations) distribution of pressures along the array for a source centered on the array are shown for the parallel (C) and perpendicular (D) orientations illustrated in A and B (thick solid lines). The instantaneous spatial pattern from arrayed sensors (thick lines) in C and D are similar to the temporal response pattern from a single sensor (hydrophone; thin lines with symbols) to a dipole source that travels along a linear transect some distance from the source center (in this case, 2 cm). Also shown are the predicted changes in the phase angle or polarity (pressure above or below ambient) of the response (dashed thick lines). For the parallel case in A, the peak pressure reaches a null at x=0, coincident with a 180 deg shift in the phase angle. By contrast, the peak pressure reaches its maximum value at this location for the perpendicular case and the polarity remains the same throughout. The corresponding particle motion (not shown) reaches a maximum at x=0 for the parallel case, but a null at this location for the perpendicular case.

the responses of the auditory system to fine-scale, spatiotemporal changes in both pressure and particle motion. Moreover, the orientation of the dipole can be manipulated to produce dramatic differences in the overall spatial distribution of pressures to test the degree to which pressure drives any given response (see Fig. 1).

In this study, we test the hypotheses: (1) that saccular, but not lagena, responses are governed by pressure inputs to the ASB; and (2) that pressure information about the changing position and orientation of dipole sources is encoded by the saccule. If saccular nerve fiber responses are driven by pressure inputs to the ASB, then the neural response patterns should match those modeled and measured for a pressure sensor in the same relative location as the ASB, and should additionally be altered after ASB deflation. In addition, we use conditioned suppression of respiration to measure the behavioral response of goldfish to the same source at different locations along the length of the fish. Comparisons of behavioral, neural and hydrophone response patterns reveal that saccular but not lagenar nerve fibers faithfully encode both the polarity and amplitude of pressure at the ASB, and that behavioral responses to different locations and orientations of the 50 Hz dipole are dominated by pressure inputs to the sacculi from the ASB.

MATERIALS AND METHODS

Experimental animals

Goldfish (*Carassius auratus*) used in both neurophysiological and behavioral experiments were obtained from local commercial suppliers and maintained at the Loyola University Chicago in 20 gallon communal tanks for the duration of the project. All goldfish were kept at 12–14°C. Individuals were 8–13 cm in standard length. The care and treatment of fish were approved by the Animal Care and Use Committee of Loyola University Chicago.

Stimulus generation and measurement

The dipole source used in neurophysiological and behavioral experiments consisted of a small (6 mm in diameter), sinusoidally oscillating (50 Hz) plastic sphere rigidly attached to a minishaker (B and K 4810) by a stainless steel, blunt-tipped needle (16 gauge, 12 cm in length). The shaft (needle) was mounted perpendicular to the axis of diaphragm motion and the long axis of the shaker. The shaker was then suspended above the experimental tank so that the driving shaft extended downwards into the water to produce sinusoidal oscillations of the dipole in the horizontal plane along a rostral-caudal axis relative to the submerged fish or hydrophone (Fig. 2). The amplitude and frequency of oscillation were computer-controlled through a Tucker-Davis Technologies (TDT) D/A module. The sinusoidal signal was gated on and off at 0 deg starting phases to produce a series of 50 Hz pulses (500 ms on, 500 ms off), each with 10 ms rise/fall times.

For neurophysiological experiments and stimulus measurement, the location of the dipole source was continuously changed at the rate of 4 mm/s along a single linear axis parallel to the longitudinal axis of the fish (Figs 1, 2) while recording the evoked activity from auditory or lagenar nerve fibers and, in separate trials, the voltage output of the hydrophone. For behavioral experiments, the dipole

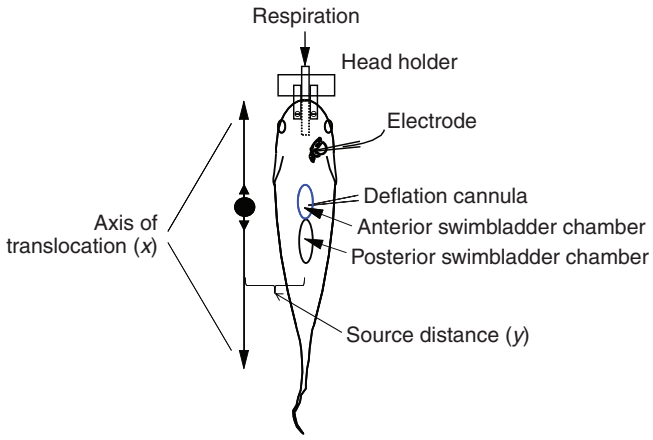

Fig. 2. Schematic diagram of the stimulus delivery system, and the relative position of the fish and dipole source during both neurophysiological and behavioral experiments. Various design features of the neurophysiological experiments are also illustrated, including the head holder with flow tube to artificially respirate the fish, electrode placement on the auditory (saccular) nerve in the cranial cavity, and the use of a cannula to deflate the anterior swimbladder chamber.

source was kept in a stationary position at a given location along the length of the fish for each behavioral measurement and then randomly moved to several different locations along the fish during the same test session. In addition, the dipole axis of vibration was varied between one that was parallel to the long axis of the fish (Fig. 1A) and one that was perpendicular to the fish's long axis (Fig. 1B). All of the positions together formed a linear transect that was similar in elevation, distance to the fish, etc., as the continuous transect used in neurophysiological experiments. Dipole positioning was accomplished by mounting the minishaker to a sliding plate, moved by a worm-gear assembly (Velmex, Bloomfield, NY, USA) that was driven by a stepper motor under computer control. This assembly was in turn mounted on independently controlled x, y and z assemblies that enabled precise positioning of the source (relative to the fish or hydrophone) in all three dimensions.

The sound pressure associated with the changing locations of the dipole source was measured with a miniature hydrophone (model 8103, Brüel and Kjaer), at the same elevation as the dipole and positioned at the middle of the x-axis range of linear motion at varying distances (y axis) from the fish or hydrophone. Measurements were made in the experimental test tank at the same submerged location as the fish's anterior swimbladder chamber, but in the absence of the fish. The time-waveform of the hydrophone output was digitized (TDT A/D module) and used to compute the average root-mean-square (RMS) amplitude over each 2 mm segment of linear motion. The amplitude spectra and instantaneous frequency were also obtained from a fast Fourier transform of the digitized waveform and both the spectrum and the waveform were inspected to ensure that sphere oscillations were sinusoidal with dominant energy at 50 Hz. Because this study focused primarily on the role of pressure-driven inputs to the ear via the ASB, direct measurements of particle motions were not made.

Computational modeling

As illustrated in Fig. 1, the spatial distribution of pressure was modeled at 2 mm intervals along a linear transect 1–2 cm away from a dipole source using the flow-field equations for a dipole source in a spherical coordinate system (Morse, 1948; Harris and van Bergeijk, 1962; Kalmijn, 1989; Coombs et al., 1996). The flow-field calculations were based on a 'snapshot' in time when the source is at its furthest positive excursion. MATLAB (Version 4.0, The Mathworks, Natick, MA, USA) was used to program the equations for a dipole source of the same size and stimulus dimensions as those used in the neurophysiological experiments (see stimulus generation). Pressure amplitude (p) was calculated as:

$$p(r,\theta) = -\frac{\rho\omega\, a^3 U_0 \cos\theta}{2r^2}\ , \qquad (1)$$

where ρ is the ambient density, $\omega=2\pi f$, r is the radial distance from source center, θ is the angular deviation from the axis of dipole oscillation, a is the dipole source (sphere) radius, and U_0 is the source velocity, arbitrarily set to 1 m s^{-1}.

Neurophysiological methods

Surgical preparation

The surgical procedure for exposing the right saccular and lagenar nerve branches has been described in detail elsewhere (e.g. Fay and Ream, 1986), but the essentials will be summarized here. Fish were anesthetized [0.01% tricaine methanesulfonate (MS-222) dissolved in tank water], immobilized with an intramuscular injection of flaxedil (0.1 mg/gm body weight) and fitted with a respirator tube, before being cradled in a small styrofoam chamber that held the fish while the cranium over the medulla and cerebellum was removed. Upon completion of the surgery, the anesthetized fish was transferred to a rectangular Plexiglas test tank (16.5×17.8×36.8 cm) filled with recirculated, chilled and aerated fresh water. The fish's head was clamped onto a custom-made respirator/head holder with screws to press the skull down onto a brass respirator tube in the fish's mouth. The dorsal portion of the cranium was positioned above water, but the trunk of the fish was submerged with the tail down at a slight (10–20 deg) angle from the horizontal, such that the ASB was submerged below the water surface by about 1–2 cm. The experimental tank rested on a TMC pneumatic vibration isolation table inside a small, single-walled IAC (Industrial Acoustics, Bronx, NY, USA) sound-attenuating booth.

The right saccular and lagenar nerves were exposed by gently retracting the cerebellum and the vagus lobe of the medulla. The saccular nerve exits the saccule and courses dorsally, anteriorly and laterally to its point of entrance to the medulla at the descending octaval nucleus. The lagenar nerve exits more laterally and posteriorly through a foramen in the bone overlying the lagena. The lagenar nerve joins the saccular nerve as it enters the medulla about 0.5–1.0 mm anterior of the foramen. For this study, we recorded from cells in the main trunk of the saccular and lagenar nerves within 0.5 mm of their exiting their respective endorgans, and posterior to the location where these two branches of VIII join at their entrance to the medulla. In every recording experiment, both nerve branches were visualized so that it was possible to record from one or the other without ambiguity.

Neural response measure and data analysis

Micropipettes filled with 3 mol l^{-1} KCl (impedance ranging from 10 to 50 MΩ) were placed on the saccular or lagenar nerves with a micromanipulator and advanced through the nerve with a motorized microdrive. The output of the microelectrode was amplified within a 300 to 3000 Hz bandwidth, and single spikes were distinguished by a voltage-level discriminator that converted them into TTL pulses. Data acquisition components of a modular hardware system (TDT) recorded TTL pulses in the form of elapsed times from stimulus onset to the occurrence of the TTL pulse.

Evoked activity was recorded in response to a dipole source that slowly changed its position in a head–tail and then a tail–head direction for five repetitions in each direction (Fig. 2). Source amplitudes were initially varied to span the dynamic range of the afferent fiber. The data displayed here (see below) were selected from those source amplitudes that were in the approximate center of the dynamic range. The axis of oscillation was kept parallel to the long axis of the fish (in the x-axis) for all neurophysiological response measurements (Fig. 1A). Because the x-axis of motion had to be kept perfectly horizontal to assure smooth operation of the worm gear, the axis of dipole motion (linear translation) and oscillation was not perfectly parallel to the long axis of the fish, which angled downward by a small amount from the horizontal surface of the water. Similarly, although the distance of the source was set to 1–1.5 cm from the midline of the fish at the snout, the distance to the fish's body surface could vary slightly along the length of the fish owing to the curvature of the fish's body.

Neural responses to the changing locations were summarized in a spatial event plot (SEP) that relates the change in responsiveness to the x-position of the source. To ensure that neural response patterns were governed primarily by source location and not by other factors, such as the slow linear motion, we also ran three control conditions when time permitted: sinusoidal oscillation of the sphere in the absence

of linear motion, linear motion in the absence of oscillation, and the absence of both oscillation and linear motion.

Neural responsiveness was measured for each 500 ms pulse (=25 sinusoidal cycles or 2 mm of travel) to yield location-specific measurements of (1) the average firing rate (spikes s^{-1}), (2) the average phase angle of spike times with respect to the signal to the minishaker and (3) the Raleigh statistic, *Z*. Both the phase angle and *Z* were determined by collapsing elapsed spike times into a single period histogram and determining the phase angle and length of the mean histogram vector, *R* (Goldberg and Brown, 1969). The Rayleigh *Z*-statistic was calculated as $Z=R^2\times N$, where *N* is the total number of spikes (Batschelet, 1981). Response values at each location were then averaged over five repetitions of movement in each direction.

The *Z*-statistic was used in two ways: (1) as a combined measure of firing rate and phase-locking to the sinuosidal stimulus; and (2) as a statistical test of whether or not phase-locking and phase angle measures were drawn from a uniformly distributed sample population (i.e. the period histogram). *Z*-values above about 4.6 indicate that the probability of the period histogram being uniform was less than 0.01 [see table 4.2.1 from Batschelet (Batschelet, 1981)]. In this paper, we assume that phase angles associated with a *Z*-statistic of <4.6 are not reliable and, thus, exclude the associated *Z*-values from graphic displays and analysis.

To deflate the swimbladder, a fine-gauge needle was inserted into the anterior swimbladder chamber through the dorsolateral musculature, and the gas in the swimbladder was withdrawn with a syringe attached to the needle via a short length of micro-tubing (see Fig. 2). This method allowed us to measure the volume of gas that was removed from the bladder and to confirm deflation.

After the end of each experiment, fish were deeply anesthetized in MS-222 and the trunk skin and musculature were dissected away to reveal the ASB and to determine the extent to which it had been deflated. In addition, the distance between the fish's snout and the rostral end of the ASB was measured, as was the rostrocaudal length of the ASB.

Behavioral methods

Classically conditioned suppression of respiration (Fay, 1994) was used to measure behavioral responsiveness of goldfish (8–9 cm in length) to a dipole source [of the same diameter (6 mm) and vibration frequency (50 Hz) as those used in physiological experiments] as a function of (1) rostrocaudal location along the length of the fish and (2) source orientation (parallel or perpendicular to the long axis of fish; compare Fig. 1A with 1B). For testing, fish were placed in a 45 cm wide by 28 cm high cylindrical tank that was isolated from substrate vibrations by a Micro-G pneumatic system and from ambient sounds by a single-walled, sound-attenuating IAC chamber. Fish were loosely held in place and suspended below the water surface in a fine-filament (~0.2 mm) and wide-mesh (3 mm bore) bag that permitted stimulation of both the lateral line and the auditory system. A thermistor in front of the fish's mouth measured the amplitude and rate of respiratory flow during signal and blank trials of equal duration. Fish were conditioned to reduce their respiration rate during a 7 s series of dipole vibrations (500 ms on, 500 ms off) by following the stimulus with a mild electric shock (2–5 V at the source, 250 ms in duration), which caused an unconditioned reduction in respiration lasting from 1 to 3 s. After 10 to 20 conditioning trials, the vibration of the sphere tended to cause a conditioned response of respiratory suppression. The respiration rate occurring during the 7 s interval preceding the stimulus trial was compared to the rate during the stimulus trial to yield a measure of the percentage suppression, where 100% represented complete suppression and 0% corresponded to cases in which the respiration activity to the stimulus trial was greater than or equal to that measured in the preceding 7 s period without any stimulus.

Testing consisted of two phases. Initial tests for each fish generated a psychometric function in which response magnitude (percentage respiratory suppression) was measured as a function of stimulus amplitude for a single source location. The source was located at one of two locations predicted (from computational models) to produce maximum pressure levels at the ASB when the source orientation (vibration axis) was parallel to the long axis of the fish. During the second phase of testing, fish were presented with nine signal trials from different source locations over a 30 cm range, keeping source amplitude, distance from fish midline (2 cm) and orientation fixed; the series was repeated four times in random orders of location for each daily session to yield a daily response function based on four signal trials/location. All signal trials were followed with the shock. Source amplitude for the second phase was set to a suboptimal level near the top of the each individual's psychometric function. This ensured that responses fell below the saturated range of the psychometric function (<100%) and were free to vary over the entire dynamic range.

RESULTS

Computational modeling and stimulus measurement results

For the source orientations and iso-pressure contours depicted in Fig. 1A,B, the spatial distribution of computed (modeled) peak pressures is re-plotted in Fig. 1C,D in 2 mm intervals (solid black line, left axis) to reflect the expected distribution of activity along a linear array of pressure sensors. These figures illustrate that peak (absolute) pressures at a single moment in time vary in spatially complex ways that are dependent on the orientation of the source with respect to the sensor array.

In addition, the switch in pressure polarity (pressure above or below ambient) observed at the center of the array (directly opposite the source) for a dipole vibration axis that was parallel to the array is represented as an abrupt 180 deg change in the phase angle or preferred response time of the pressure sensors (Fig. 1C, dashed black line, right axis). The 180 deg shift assumes that all sensors in the array have the same preferred response time (e.g. hair cells all oriented to respond best to the compression of the ASB during the positive-pressure phase of each cycle), but that for any given moment in time, roughly half of the hypothetical sensors (i.e. those in front of the advancing source) experience compression and displacement in one direction, whereas the other half (those in the rear of the advancing source) experience rarefaction and displacement in the opposite direction. In contrast to the parallel orientation illustrated in Fig. 1A,C, the perpendicular orientation illustrated in Fig. 1B,D exhibits no 180 deg changes in pressure polarity.

These plots illustrate the instantaneous 'spatial pattern' of pressure amplitudes and polarities along an array of sensors and, in this case, the appropriate *x*-axis label in Fig. 1C,D is 'sensor location re: source'. However, the same plots can also be used to make predictions about the 'temporal pattern' of responses that would be expected from a 'single sensor' to a source that changes its position along a linear transect (i.e. the length of the fish) – in which case, the appropriate *x*-axis label is 'source location re: sensor'. Indeed, the measured response of a single hydrophone to a slowly traveling dipole source confirms the modeled expectations, as shown in Fig. 1C,D (thin lines with symbols).

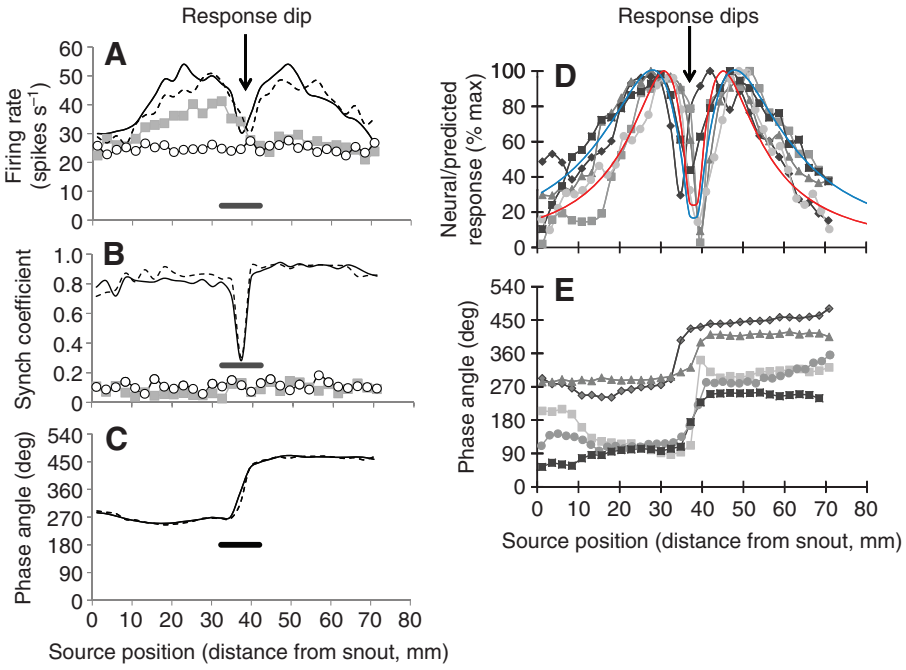

Fig. 3. Spatial event plots illustrating the firing rate (A), synchronization coefficient (B) and phase angle (C) response of a Type 1 saccular fiber as a function of source location along the length of the fish, and for two control conditions (see below). Note that phase angles are plotted here and elsewhere as varying from 0 deg to 540 deg. This convention was used to illustrate accurately phase lags that likely 'wrapped' or exceeded the unit cycle, crossing the 360 deg limit. In these cases, the phase was calculated as a lag that was greater than 360 deg, rather than one close to 0 deg. Response amplitudes (D) and phase angles (E) from different saccular fibers and multiple individuals are also shown. In D, neural responses are co-plotted with modeled predictions for sources that are either centered in elevation on the sensor (red lines) or elevated by 1 cm (blue lines). The spatial extent of the ASB is delineated by the thick bar in panels A–C. In A and B, responses from two directions of travel (rostrocaudal, solid lines, and caudal-rostral, dashed lines) are shown for three stimulus conditions: (1) stimulus condition in which the dipole source is vibrating and slowly changing its location along the fish (dashed and solid lines for head–tail and tail–head sweep directions, respectively); (2) control condition in which the dipole source moves along the fish but does not vibrate (gray line with solid squares, mean of data from both sweep directions); and (3) the final control condition in which the source neither moves nor vibrates (black solid line with open circles, mean of data from fictive sweeps in both directions). Phase angles for control conditions are not plotted in C because period histograms were judged to have uniform distributions, based on *Z*-statistic values (see Materials and methods). Response amplitudes in D are characterized by the *Z*-statistic metric (number of spikes × synchronization coefficient squared, see Materials and methods), which has been averaged across rostrocaudal and caudal-rostral directions of travel. Modeled and measured response patterns have been horizontally shifted to make response valleys coincide with neural response valleys.

Neurophysiological results

Useable results (complete spatial event plots) from normal animals (no swimbladder deflation) were obtained from 30 saccular fibers in nine individuals and from 18 lagena fibers in three individuals. Among these individuals, the rostrocaudal length of the inflated ASB chamber ranged from 7–18 mm (mean=12.9±2.92 mm). The center of the ASB chamber was situated 35–52 mm from the tip of the snout (mean=41.9±4.7 mm). The ASB location (distance of the ASB center from snout) was significantly correlated with standard body length (R^2=0.73, P=0.0004) and was nearly a fixed fraction of standard length (SL; mean=0.43±0.03 SL).

Response patterns of saccular fibers to the changing positions of the dipole source fell into two categories, depending on the number of observed peaks and valleys in the overall pattern. Type 1 patterns (17 fibers in six fish) were characterized by two firing-rate-response peaks: one in response to source locations ~10–15 mm rostral to the ASB and the second to locations ~10–15 mm caudal to the ASB (Fig. 3A). The two response peaks were separated by a single, prominent drop in both the average firing rate (Fig. 3A) and the synchronization coefficient (Fig. 3B) when the source was opposite the ASB. This response dip or valley was also accompanied by an abrupt shift in the phase angle (Fig. 3C). The overall pattern of response was independent of the direction of travel for all three response measures (Fig. 3A–C, solid and dashed lines without symbols).

Type 1 response patterns were observed in 17 saccular fibers in six different individuals (Fig. 3D,E). Moreover, neural response patterns matched the modeled predictions quite well, falling within the range of predictions modeled for two extremes: (1) when the source and the ASB are at the same elevation (red function in Fig. 3D); and (2) when the source was higher or lower in elevation than the ASB by 1 cm (blue function in Fig. 3D). The range in modeled patterns due to different source elevations was also similar to that generated for a narrow range of source distances (~1–1.5 cm) for a source elevation centered on the array. Computational models for pressure patterns also predict that pressure valleys, associated with the center of the dipole moment, coincide with abrupt, 180 deg phase-shifts (Coombs et al., 1996) (Fig. 1D). This shift results when the pressure receiver registers a switch in the order of compression and rarefaction phases during any given sinusoidal cycle, as happens when the source travels past the receiver and the sound pressure produced is minimal. If the sensor 'experiences' compression first and rarefaction second as the source approaches, it will then experience rarefaction first and compression second after the source moves past it and further away. The sensing order is reversed when the source is directly

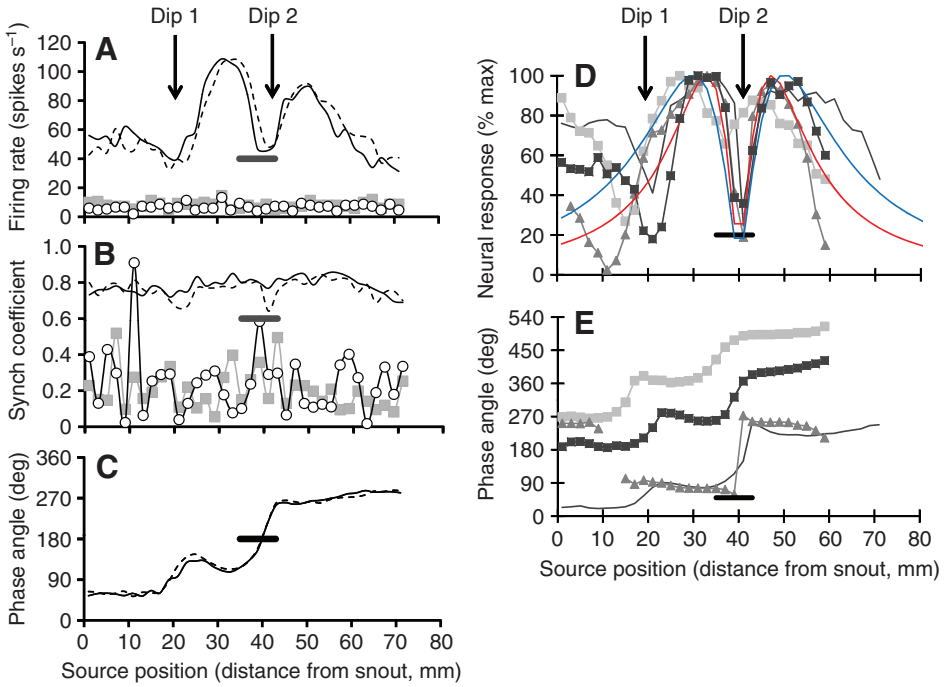

Fig. 4. Spatial event plots (as in Fig. 3) illustrating a typical 'two-valley' (Type 2) response from a single saccular fiber in which the first response valley (A) and corresponding phase shift (C) occurs when the dipole source is near the head, ~20 mm behind the snout, and the second when the source is in the vicinity of the ASB (thick bar). Additional examples are shown in D and E from saccular fibers in different individuals (gray and black lines), as compared with modeled predictions for pressure distributions (red and blue functions) at two source elevations (0 and 2 cm, respectively). See Fig. 3 for additional details on response measures and stimulus conditions.

opposite the receiver, resulting in an abrupt 180 deg shift in the phase angle at this source location.

Type 2 patterns (13 fibers in three fish) differed from Type 1 patterns by having two response dips (Fig. 4A,B) and corresponding phase shifts (Fig. 4C). The first dip occurred for source locations near the head, ~10–20 mm behind the snout (hereafter referred to as the 'head location') and the second for source locations adjacent to the ASB (hereafter referred to as the 'ASB location'). As with Type 1 responses, the overall pattern of response was independent of the direction of travel (Fig. 4A–C, solid vs dashed lines) and was observed in several different fibers and individuals (Fig. 4D,E). However, not all features of Type 2 patterns were a good match for the modeled predictions of pressure-reception by the ASB. That is, the first response dip, caused by source locations near the head, could not be predicted by pressure models, whereas the second dip, caused by ASB source locations, and its surrounding response peaks were a fairly good, but not perfect match to the pressure predictions (Fig. 4D).

Among saccular fibers held long enough to run all control conditions, some, but not all, Type 1 fibers (five fibers from two fish) exhibited responses to the translational movement of a non-vibrating dipole, as illustrated by the fiber in Fig. 3A (functions with solid gray squares). Firing-rate responses to the movement alone were substantially above the rates measured when the dipole source remained stationary without vibrating (functions with open circles in Fig. 3A), but below those elicited by both movement and vibrations combined (dashed and solid lines in Fig. 3A). Firing-rate-response patterns to movement alone were asymmetric, showing greater responsiveness for source locations rostral to the ASB, regardless of the direction of travel (Fig. 3A, solid gray squares). By contrast, Type 2 fibers (N=2 from one individual) failed to show responses to either of these directions of movement in the absence of vibration (Fig. 4A, solid gray squares).

Lagenar fibers had response patterns that were in part similar to Type 2 saccular fibers in that there were prominent response valleys and corresponding phase-shifts for source locations in a narrow region along the head, ~20–25 mm behind the snout (Fig. 5). However, there was no evidence for response valleys or phase shifts at ASB source locations, as would result from responses driven by pressure inputs to the ASB. Phase angles for source locations anterior and posterior to that causing the phase shift remained relatively constant. Lagenar fibers exhibited no responses to control conditions (Fig. 5A,B).

The frequency distributions of response valley and phase-shift locations for saccular fibers (Type 1 and 2 combined) were bimodal (see Fig. 6), with the majority of response valley/phase-shift locations being centered on the ASB and a minority in the vicinity of the saccule, which was approximately 2 cm rostral to the ASB (Fig. 6A,B). By contrast, lagenar distributions were uni-modal with response valley/phase-shift locations in the vicinity of the lagena, at distances a little less than 2 cm rostral to the ASB (Fig. 6C,D). Response-valley locations were highly correlated with phase-shift locations for saccular fibers (R^2=0.99; Fig. 6E, gray plus symbols), but less so for lagenar fibers (R^2=0.42; Fig. 6E, open circles). Source locations near the head associated with response valleys and phase shifts in lagenar fibers (open circles, Fig. 6E) appeared to be slightly caudal to those of saccular fibers (plus symbols, Fig. 6E).

Effects of swimbladder deflation and vibration frequency on response patterns

Experiments to observe the effects of ASB deflation yielded useable results from a total of 24 saccular fibers in five individuals and 16 lagenar fibers in three individuals. For initial experiments, pre-

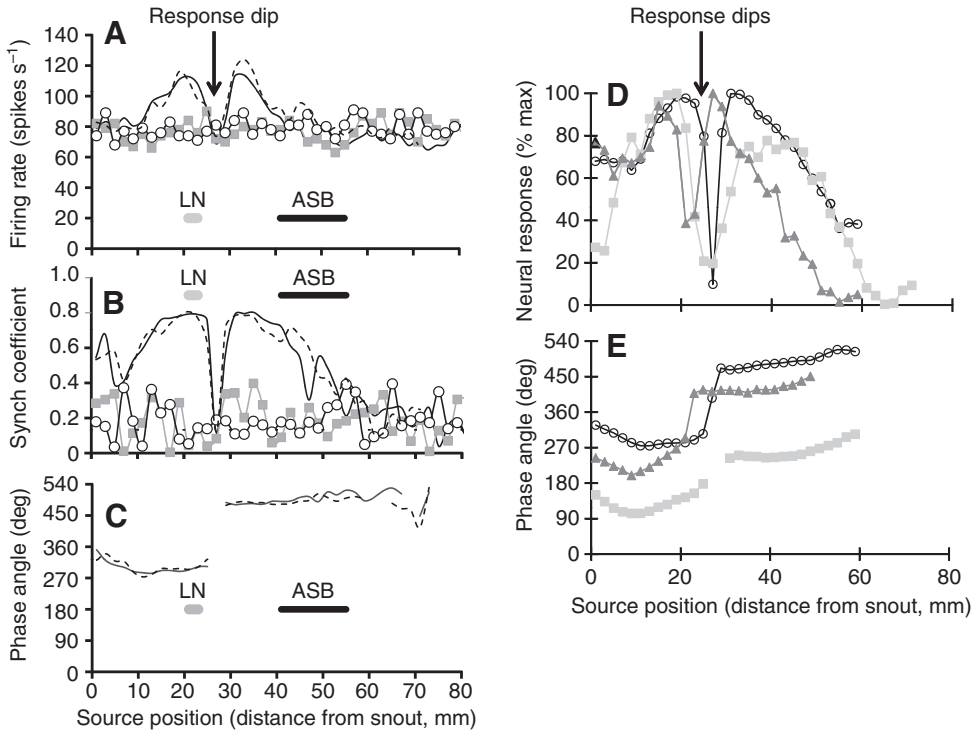

Fig. 5. Spatial event plots (as in Figs 3 and 4) for a single lagenar fiber (A–C), showing a single response valley at the head (x=~25 mm; A,B), nearly 2 cm rostral to the ASB (thick bar) location. Additional examples are shown in D and E from lagenar fibers in different individuals (gray and black lines). See Fig. 3 for additional details on response measures and stimulus conditions.

deflation recordings were done in individuals with a cannula implanted in the ASB so that pre- and post-deflation results, as well as re-inflation results, could be collected from the same fiber. In many of these cases, pre-deflation results with the cannula inserted appeared to be abnormal. For example, four saccular fibers from one fish exhibited a pattern that had one valley at the head location only – a response that was never observed in normal fish. Accordingly, later experiments measured between-fiber differences within an individual before and after the cannula had been inserted. Results from both approaches were consistent in showing that deflation of the ASB reduced firing-rate levels and phase-locking abilities of saccular fibers. To illustrate these effects, spike rate

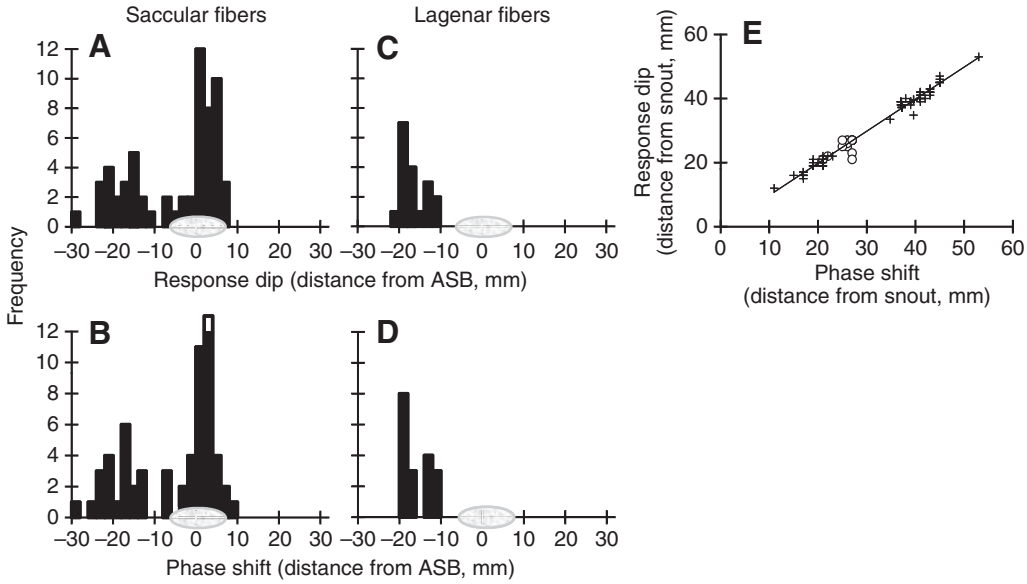

Fig. 6. Frequency distributions of source locations corresponding to response amplitude valleys (A,C) and phase-shifts (B,D) for all saccular (A,B; N=30) and lagenar (C,D; N=18) fibers. Each amplitude valley and phase shift value is based on the mean of values obtained for rostrocaudal and caudalrostral directions of movement. In E, the relationship between response amplitude valley and phase shift location is plotted for each saccular (crosses) and lagenar (open circles) fiber. Note that results in A–D are plotted in terms of distance from the center of the ASB; negative numbers indicate that the response dip or phase shift occurred for source locations rostral to the ASB, whereas positive numbers indicate that source locations were caudal to the ASB. By contrast, results in E are plotted in terms of distance from the snout. In both cases, left is in a headward direction, right is in a tailward direction. Results were taken from fish that varied in standard length from 77 to 130 cm.

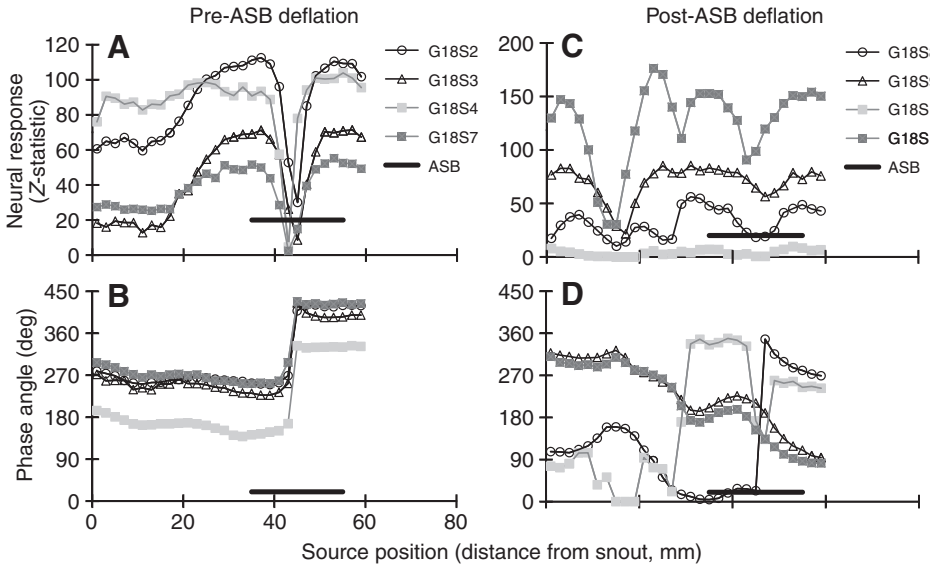

Fig. 7. Between-fiber effects of ASB deflation. Spatial event plots of mean *Z*-statistic (A,C) and phase-angle (B,D) responses of different saccular nerve fibers in the same individual before (A,B) and after (C,D) deflation of the ASB.

(number of spikes, *N*/s) and synchronization coefficients (*R*) were combined into a single metric, the *Z*-statistic ($N \times R^2$; see Materials and methods), and plotted as a function of source location (Fig. 7). Between-fiber results within the same individual were similar to within-fiber results. That is, before deflation, the majority of saccular fibers from any given fish had Type 1 response patterns with prominent response valleys (Fig. 7A) and phase shifts (Fig. 7B) at the ASB source location (thick bar). After deflation, response peaks and valleys at the ASB location were generally diminished (Fig. 7C). Moreover, the overall response pattern of some post-deflation fibers (e.g. G18S9 and G18S16) took on the appearance of a Type 2 response with an additional response valley (Fig. 7C) and phase-shift (Fig. 8D) occurring for head locations of the source (~18–20 mm behind the snout).

By contrast, ASB deflation had little to no effect on the magnitude or location of the response valleys recorded from lagenar fibers (Fig. 8). Post-deflation response peaks appear somewhat flattened, but this is only because the fibers were responding in the saturation range of their input/output functions. Normally, the vibration amplitude would be adjusted downwards to prevent this from happening, but we were unable to hold these fibers long enough to run additional stimulus sweeps at lower stimulus amplitudes. Nevertheless, fibers continued to show robust responses with a single response valley and phase-shift at the same head location. The source locations at which valleys and phase-shifts occurred were not significantly different between pre- and post-deflation fibers (*t*-test, unequal variances, $P>0.05$).

Although not an explicit goal for these experiments, we were able to examine the effects of vibration frequency on saccular response patterns in one individual. Several fibers in this particular individual exhibited Type 2 response patterns to the 50 Hz signal (Fig. 9A,B). However, when the frequency was increased from 50 to 100 Hz, the same fibers exhibited a Type 1 response pattern (Fig. 9C,D).

Behavioral results

Despite intra-individual variation in daily response behavioral functions (thin solid and dashed lines in Fig. 10), all individuals

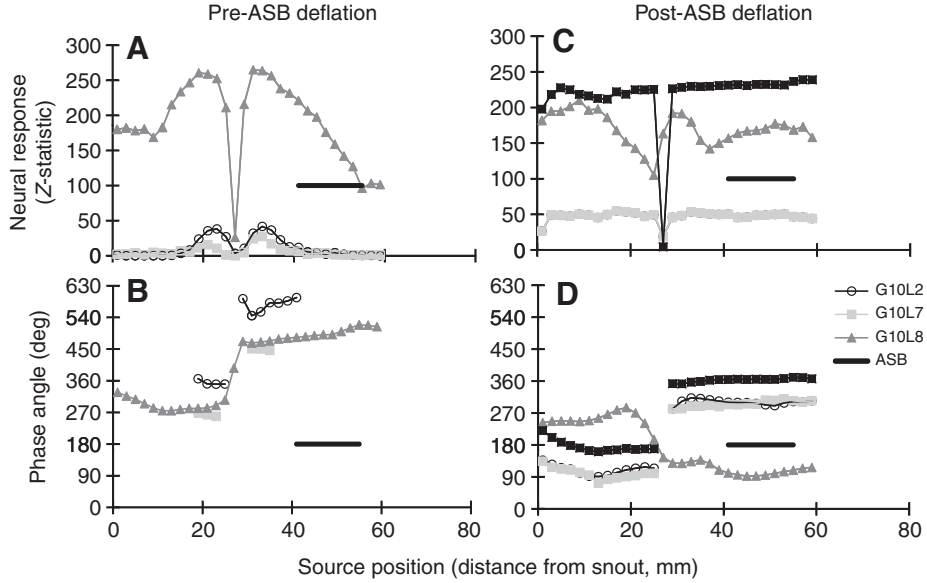

Fig. 8. Spatial event plots of mean *Z*-statistic (A,C) and phase-angle (B,D) responses of different lagenar nerve fibers in the same individual before (A,B) and after (C,D) deflation of the ASB. Note that fiber responses after ASB deflation fail to show the typical, 'rounded' response peaks that flank the response valley (compare C with A). However, this is essentially an artefact of the fiber firing in the saturated range of its input/output function. In these cases, fibers were not held long enough to determine an optimum vibration amplitude that fell below saturation levels.

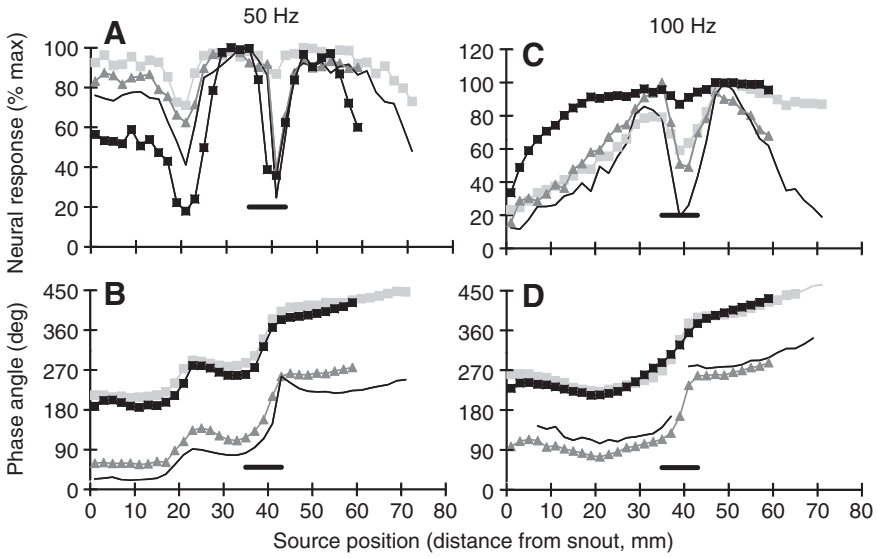

Fig. 9. The effect of vibration frequency on response type in saccular fibers from one individual. Mean *Z*-statistic (A,C) and phase angle (B,D) reponses are plotted as a function of source location and frequency. Each symbol represents the same fiber in all Four panels. Spatial event plots for each of four different fibers switch from exhibiting two valleys at 50 Hz (one at the head and one at the ASB, as indicated by the black horizontal bar; A,B) to one valley only (at the ASB; C,D) at 100 Hz.

exhibited mean response functions (thick solid line in Fig. 10) with similar characteristics. When the vibration axis was parallel to the long axis of the fish in a head–tail direction (Fig. 10, right panels), response functions exhibited a valley for source locations in the vicinity of the ASB (thick bar in Fig. 10). When the vibration axis was perpendicular to the fish in a left–right direction, response functions exhibited a peak for source locations in the vicinity of the ASB (Fig. 10, left panels). Pre- and post-session measurements of snout position revealed that the position of the fish in the restraining bag sometimes shifted during the session. Shift magnitudes were small, however, ranging from 0 to 4 mm in any given (*x*, *y* or *z*) dimension and averaging less than 0.5 mm.

DISCUSSION

ASB pressure inputs to the saccule for the detection of dipole positions

The results of this study confirm and extend the findings of earlier reports (Fay, 1969; Coombs, 1994; Daily and Braun, 2009) in showing that the goldfish auditory system responds to nearby, low-frequency dipole sources and that pressure inputs to the auditory system dominate behavioral detection at low frequencies. In addition,

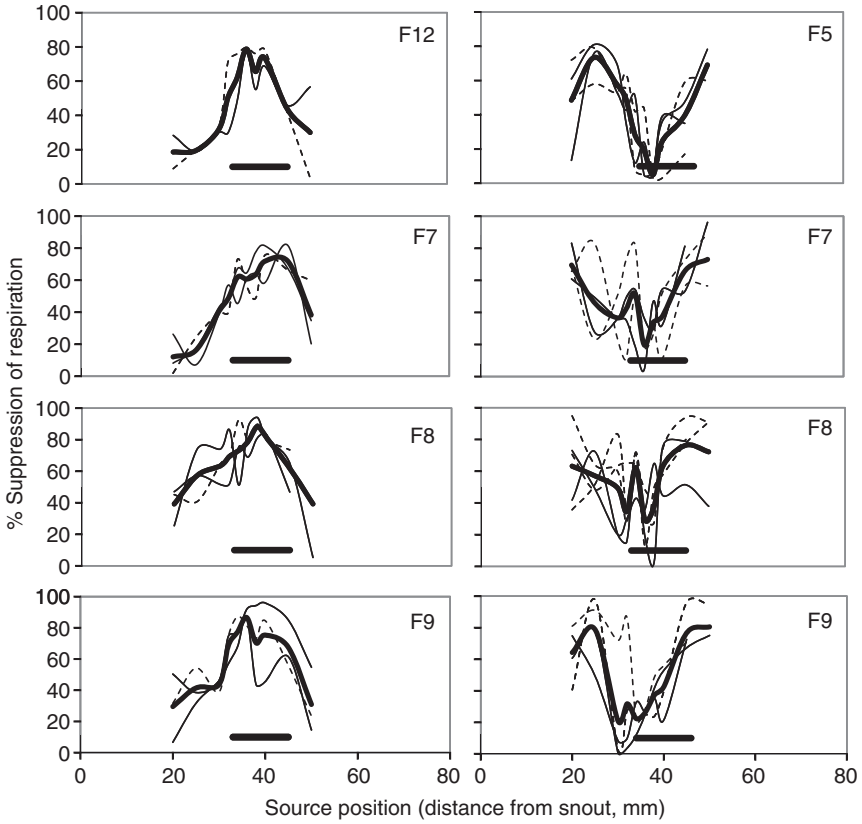

Fig. 10. Spatial event plots of conditioned behavioral responses in four individuals to a dipole source at different locations along the fish. Each thin line represents data collected during a single daily session (four signal trials for each of nine source locations), whereas thick lines represent the mean of daily sessions. In left panels, the axis of vibration was perpendicular (head–tail) to the long axis of the fish, whereas in right panels it was parallel (left–right).

this study provides new evidence that responses of the inner ear saccule, but not the lagena, are governed by local pressure inputs to the ASB. As a relatively small and localized pressure receiver, the ASB is thus able to register the local pressure changes associated with small changes in the location of the source relative to this body-centered receiver. The mean length of the ASB chamber (12.9 mm) for fish in this study was only slightly bigger than the diameter of the mini-hydrophone (9.5 mm) used for stimulus measurements. When compared with modeled predictions based on 2 mm intervals, both the mini-hydrophone and the ASB chamber appeared to be capable of faithfully registering small changes in pressure associated with source locations that differed by only a few millimeters.

A number of studies have now shown reasonably good agreement between modeled predictions and measured pressure and/or particle motion levels surrounding small dipole sources in small tanks (Denton and Gray, 1982; Coombs et al., 1989; Coombs et al., 1996; Yang et al., 2006). Thus, it appears that the modeling assumptions of these studies (unbounded, free field conditions) are quite reasonable, even though experiments were conducted in small tanks bounded by walls and an air/water interface. Boundary-created distortions might be negligible under these circumstances, because source amplitudes were relatively small (sphere displacement <0.1 mm) and because nearfield pressure and particle motions decline at very steep rates ($1/R^2$ and $1/R^3$, respectively).

Source positions near the ASB clearly modulated conditioned suppression of respiration in a manner that could be predicted by corresponding changes in pressure inputs to the saccule as a function of both source location and orientation (Figs 10, 11). Slight irregularities (bumps and dips) in behavioral response functions were most likely caused by shifts in the position of the fish in the restraining bag. Measured shifts were quite small (<4 mm), but even small changes in the relative location of the sensor (i.e. the ASB of the fish) could have large impacts on the received pressure magnitudes if the sensor was opposite the source and in the region of the pressure null (Fig. 1A), as would be expected for source locations near the ASB.

The extent to which dipole sources guide natural, unconditioned behaviors in goldfish remains unclear, largely because appropriate bioacoustic behaviors for study have yet to be identified as they have been for the mottled sculpin (*Cottus bairdi*). For these benthic fish, small, low frequency dipoles elicit an unconditioned, prey-orienting response that is completely eliminated when the lateral line system is blocked (Hoekstra and Janssen, 1985; Coombs et al., 2001). By contrast, conditioned suppression of respiration to the same dipole source is unaffected in this species when the lateral line system is blocked, suggesting that different sensory modes dominate in different behavioral contexts (Braun and Coombs, 2010). Nevertheless, there is substantial if not complete overlap between the two sensory systems in terms of the distance range of dipole detection (Braun and Coombs, 2000), and probably for the frequency range of detection as well. Thus, factors governing simple detection are unlikely to determine which, if any, sensory mode dominates in any given behavioral context.

For the goldfish, the situation might be different, because the ASB and the Weberian ossicles greatly enhance sound pressure (hearing) sensitivity and the frequency range of detection (Fay and Popper, 1974; Fay and Popper, 1975; Ladich and Wysocki, 2003; Yan et al., 2000). Moreover, pressure in the inner nearfield of a dipole source declines less steeply with distance ($1/\text{distance}^2$) than does the pressure gradient (the stimulus to the lateral line) or particle motion (the direct stimulus to otolithic endorgans of the inner ear; $1/\text{distance}^3$) (Kalmijn, 1988). As a result, goldfish can detect a dipole of any given source amplitude at much greater distances than can fish such as mottled sculpin, which lack swimbladders and pressure-sensing abilities (Coombs, 1994). Given that goldfish can detect at least three stimulus dimensions associated with a dipole source – pressure gradients (lateral line), particle motion (lagena and possibly saccule of the inner ear) and sound pressure (saccule) – pressure inputs from the saccule would seem to provide goldfish with the best available information for simple detection tasks. As such, it would be surprising if goldfish did not rely heavily on pressure information to learn the association between the unconditioned (shock) and conditioned (dipole) stimulus in the classical-conditioning paradigm of our behavioral study. Recent studies (Nauroth and Mogdans, 2009) revealed that lateral-line-blocked goldfish also exhibit unconditioned respiratory responses (either an increase or decrease in breathing rate) to a nearby, 100 Hz dipole source in both the presence and absence of background flow. Thus, the auditory-evoked breathing response to dipole signals, whether conditioned or unconditioned, seems to be quite robust in goldfish. Furthermore, these investigators also demonstrated that yet another species of fish, the oscar (*Astronotus ocellatus*), which has a swim bladder but no specialized connections to the inner ear, also exhibits unconditioned respiratory responses to dipole signals when the lateral line system is blocked. In total, there is now evidence that species with (oscar) and without (mottled sculpin) pressure-transducing gas cavities, as well as those with specialized connections between a gas cavity and the inner ear (goldfish), are all capable of detecting nearby, low-frequency dipole sources with the inner ear. As such, dipole source detection might be a fundamental and perhaps universal capability of fish auditory systems, as has been suggested by Kalmijn (Kalmijn, 1988).

Neural response types and stimulation routes

Type 1 response patterns from the majority of saccular fibers were observed to be a good match to measured and modeled patterns for pressure-reception by the ASB chamber (Fig. 3), indicating that these fibers were stimulated through the indirect (pressure) route. That is, fiber responses could be predicted solely on the basis of the location of the dipole source with respect to the ASB chamber. A defining characteristic of these response patterns is the single, prominent phase shift and response valley for source locations directly opposite the ASB chamber (Fig. 3). By contrast, lagena fibers showed no evidence of responsiveness or response modulation when the dipole was in the vicinity of the ASB. Phase shifts and response valleys always occurred for source positions in the vicinity of the inner ear and never for those opposite the ASB (Fig. 5). In addition, a substantial number of saccular fibers showed a somewhat different (Type 2) response pattern that suggested a combination of pressure and particle motion stimulation routes. That is, phase shifts and response valleys occurred at two source locations: one in the vicinity of the inner ear, which would be expected for the direct (particle motion) stimulation route, and a second in the vicinity of the ASB, as expected for the indirect (pressure) route.

Given that goldfish were clamped to a head holder in neurophysiological experiments, conclusions about the role that the direct stimulation route plays under normal conditions, when fish are freely suspended in the water column, cannot be made. Furthermore, because there are no rational predictions possible for the axis of motions of the fish's head when restrained by the head holder, responses to direct particle motion from otolith organs lacking swimbladder input cannot be interpreted in the present study. However, there are at least two lines of evidence that point to mixed stimulation routes as an explanation of Type 2 response patterns. First,

Type 1 saccular response patterns apparent when the ASB was intact appeared to revert back to Type 2 patterns after the ASB was deflated. That is, prominent response valleys and phase shifts that occurred for source locations in the vicinity of the ASB before swimbladder deflation, switched to new source locations in the vicinity of the inner ear after swimbladder deflation (Fig. 7). At the same time, post-deflation responses were also different from Type 2 patterns in having reduced or no phase shifts/response valleys that occurred for source locations at the ASB. This is exactly the kind of result that would be expected when the direct (particle motion) mode of stimulation is no longer dominated by the indirect (pressure) mode.

A second line of evidence involves experiments in which vibration frequency was manipulated to produce Type 2 patterns in response to 50 Hz vibration and Type 1 patterns in response to 100 Hz vibrations within single fibers (Fig. 9). These frequency-dependent response differences suggest that stimulation routes are frequency dependent. These findings are similar in principle to frequency-dependent differences in behavioral sensitivities to sound, measured from fish without specialized connections to the swim bladder (Myrberg and Spires, 1980). In these studies, an unconditioned behavioral response (courtship dip) was used to measure auditory sensitivity as a function of sound frequency for several species of damselfish (*Eupomacentrus*). Pressure/particle motion ratios were manipulated in a wave tube to produce high pressure/low particle motion and low pressure/high particle motion conditions. These studies revealed that sound pressure controlled sensitivity at frequencies above 300 Hz, whereas particle motion was the relevant dimension at 100 Hz and below.

Pressure-sensitivity in goldfish appears to dominate at much lower frequencies than in damselfish, as evidenced by Type 1 saccular response patterns and behavioral response patterns to 50 Hz. This is not too surprising given the anatomical specializations for pressure-sensitivity in goldfish. Indeed, biomechanical models of the goldfish auditory system indicate that the Weberian apparatus has a significant impact on goldfish hearing – even at the low end of the frequency range of hearing (Finneran and Hastings, 2000). Nevertheless, the presence of Type 2 response patterns in saccular fibers of normal intact fish indicate that the direct (particle motion) stimulation path might contribute to responsiveness at 50 Hz and below. Interestingly, 50 Hz is the approximate cut-off frequency above which biomechanical models predict domination by the Weberian stimulation path (Finneran and Hastings, 2000). This prediction is entirely consistent with the frequency-dependent switch from Type 2 (at 50 Hz) to Type 1 (at 100 Hz) response patterns observed in saccular fibers from one individual (Fig. 9). Taken together, our results suggest that the stimulation route for some, if not all, saccular fibers might depend on both source location and frequency. At low frequencies (<~50 Hz), responses are likely dominated by (1) particle motion for source locations near the ear, (2) pressure for source locations along the trunk and caudal to the ASB, and (3) a mixture of pressure and particle motion for source locations between the inner ear and the ASB. At higher frequencies (100 Hz), responses appear to be dominated by pressure inputs to the ASB over a wide range of source locations.

Based on biomechanical models of the goldfish auditory system, Finneran and Hastings (Finneran and Hastings, 2000) concluded that there are three stimulation pathways to the goldfish ear: the direct (particle motion) path; the Weberian path, involving the mechanical coupling between the ASB and the saccule via the Weberian ossicles; and, finally, an indirect (pressure) path between the ASB and the inner ear through intervening tissues, which could conceivably impact any of the otolithic organs, including the lagena. However, our study provides no evidence in support of an indirect pressure path to the lagena, as response valleys and phase reversals were never observed in the vicinity of the ASB (Fig. 5). Rather, response valleys and phase shifts were observed for source locations in the vicinity of the inner ear, as would be predicted for the direct route of stimulation (Fig. 5).

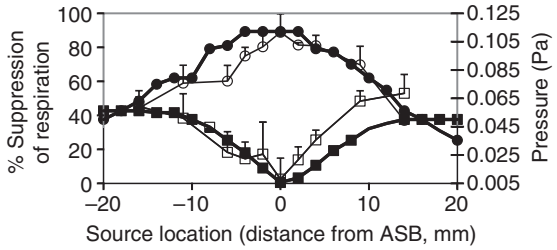

Fig. 11. Mean individual behavioral response functions (from Fig. 10; open symbols) compared with pressure levels measured from a hydrophone (filled symbols) for a 50 Hz dipole source at different positions along the fish and for both parallel (squares) and orthogonal (circles) orientations to the long axis of the fish.

The question remains as to why some, but not all, saccular fibers show evidence for dual (particle motion and pressure) stimulation routes at 50 Hz. One possible explanation is that there are regional differences in hair-cell responsiveness on the saccular macula, with some locations being more heavily influenced by pressure inputs from the ASB than others. In this regard, it is interesting to point out that source locations near the ear causing response valleys and phase shifts in saccular fibers (plus symbols, Fig. 6E) were slightly rostral to those causing response valleys and phase shifts in lagenar fibers (filled circles, Fig. 6E). Although there is considerable overlap in the rostrocaudal location of these two otolithic endorgans in the cranial cavity, the anterior-most portion of the saccule is slightly rostral to the lagena (Platt, 1977). Thus, it is conceivable that this region of the saccule, which is also that furthest away from the ASB, is less dominated by pressure inputs and thus free to respond to direct particle motion. Differentiation of the saccule into pressure and particle-motion sensing regions could, in principle, enable goldfish to extract information about both the phase and axis of source oscillation. By combining both pieces of information, 180 deg ambiguities about the direction of source motion along any given axis of motion (e.g. left or right, towards or away) could theoretically be resolved (Schuijf and Buwalda, 1975). However, it would seem that such a mechanism would work best if particle motion- and pressure-sensing channels were completely independent and uncontaminated by one another, as would be the case if pressure information from the saccule were compared with particle motion information from the lagena.

Another possibility for explaining the frequency of Type 2 responses among saccular fibers is that the relative contributions of pressure and particle motion depend on factors such as the sensitivity of the fiber, the amplitude of the stimulus relative to threshold sensitivity, and source distance. Unfortunately, we did not systematically measure the effects of any of these variables. We did manipulate source amplitude at a fixed distance and source distance for a fixed source amplitude in a limited number of cases, but observed no obvious effects on response pattern. In fact, one saccular fiber maintained a Type 2 response over a 20 dB range of source amplitudes at a source distance of 1 cm and another maintained a Type 1 response over a 4 cm range of source distances at a fixed source amplitude. Because particle-motion amplitudes decline at the

rate of 1/distance^3 in the inner nearfield of a dipole source, it is reasonable to think that particle-motion contributions to response patterns will likewise fall off rather steeply with source distance.

A third possibility is that the relative contribution of particle motion might depend on the degree to which the fish's head is rigidly attached to the head holder and on whether or not the head is free to vibrate in the stimulus field. If the head holder seriously limits the ability of otolithic endorgans to be stimulated directly *via* particle motion, then our neurophysiological results might underestimate the contribution of this stimulation route to dipole source detection and encoding. However, behavioral results from fish loosely suspended in the water column in a mesh bag suggest that this possibility is unlikely. Behavioral results are generally consistent with the conclusion that pressure inputs from the ASB/saccule receptor system dominate detection of a 50 Hz dipole over a 3 cm range of source positions. As we did not measure behavioral responses to source positions along the full length of the fish, however, we have insufficient data to fully evaluate any putative contributions of particle motion to conditioned behavioral responses.

Discriminating pressure-sensitive species from species that respond to particle motion only

Goldfish and other otophysans are well known as pressure-detecting species, whereas flatfish, sculpin and other species lacking a swimbladder (e.g. elasmobranchs) are certainly motion-sensitive species. In addition, there are other, non-otophysan species with morphological specializations of the swim bladder that are suspected to produce pressure-sensitive auditory systems (Popper and Coombs, 1982; Braun and Grande, 2008). However, the vast majority of teleosts fall into intermediate categories, responding to both pressure and particle motion to varying degrees, and in a frequency-dependent manner that depends not only on the sensing apparatus, but also on the nature of the signal and the physical characteristics of the natural environment (e.g. water depth, substrate composition, etc.) (Rogers and Cox, 1988). In all of these cases, the roving dipole procedure provides a diagnostic tool for determining the extent to which the swim bladder contributes to hearing and the degree of pressure-sensitivity.

LIST OF SYMBOLS AND ABBREVIATIONS

A	source (sphere) radius
ASB	anterior swim bladder
f	frequency
MS-222	tricaine methanesulfonate
p	pressure
r	radial distance from source center
R	length of the mean (period) histogram vector
SEP	spatial event plot
U_0	source velocity
Z	Rayleigh Z-statistic for a circular distribution
ρ	ambient density
θ	angular deviation from the axis of dipole (sphere) oscillation
ω	angular frequency

ACKNOWLEDGEMENTS

We thank Jim Finneran for the custom-written MATLAB software used in computational modeling. We are also grateful to Weihai Liu for his many contributions to behavioral experiments, including software programming and daily fish maintenance and conduction of experiments. Finally, we thank Chris Braun for his thoughtful comments and suggestions on an earlier draft of the manuscript. This work was supported by an NIDCD program project grant to the Parmly Hearing Institute, Loyola University Chicago (W. Yost, PI, S.C. and R.R.F., Co-PIs) and by an R01 grant from NIDCD (R.R.F., PI). Deposited in PMC for release after 12 months.

REFERENCES

Batschelet, E. (1981). Circular statistics in biology. In *Mathematics in Biology*, pp. 52-83. New York: Academic Press.

Braun, C. B. and Coombs, S. (2000). The overlapping roles of the inner ear and lateral line: the active space of dipole source detection. *Philos.Trans. R. Soc. Lond. B Biol. Sci.* **355**, 1115-1119.

Braun, C. B. and Coombs, S. (2010). Vibratory sources as compound stimuli for the octavolateralis systems: Dissection of specific stimulation channels using multiple behavioral approaches. *J. Exp. Psychol. Anim. Behav. Process.* **35**, 243-257.

Braun, C. B. and Grande, T. (2008). Evolution of peripheral mechanisms for the enhancement of sound reception. In *Fish Bioacoustics* (ed. J. F. Webb, A. N. Popper and R. R. Fay), pp. 99-144. New York: Springer.

Chapman, C. J. and Hawkins, A. D. (1973). A field study of hearing in the cod, *Gadus morhua* L. *J. Comp. Physiol. A* **85**, 147-167.

Coombs, S. (1994). Nearfield detection of dipole sources by the goldfish, *Carassius auratus*, and mottled sculpin, *Cottus bairdi*. *J. Exp. Biol.* **190**, 109-129.

Coombs, S., Fay, R. R. and Janssen, J. (1989). Hot-film anemometry for measuring lateral line stimuli. *J. Acoust. Soc. Am.* **85**, 2185-2193.

Coombs, S., Hastings, M. C. and Finneran, J. J. (1996). Modeling and measuring lateral line excitation patterns to changing dipole source locations. *J. Comp. Physiol.* **178**, 359-371.

Coombs, S., Braun, C. B. and Donovan, B. (2001). The orienting response of Lake Michigan mottled sculpin is mediated by canal neuromasts. *J. Exp. Biol.* **204**, 337-348.

Daily, D. D. and Braun, C. B. (2009). The detection of pressure fluctuations, sonic audition, is the dominant mode of dipole source detection in goldfish (*Carassius auratus*). *J. Exp. Psychol.* **35**, 212-223.

de Vries, H. L. (1950). The mechanics of the labyrinth otoliths. *Acta Otolaryngol.* **38**, 262-273.

Denton, E. and Gray, J. A. B. (1982). The rigidity of fish and patterns of lateral line stimulation. *Nature* **297**, 679-681.

Evans, H. M. (1925). A contribution to the anatomy and physiology of the air-bladder and weberian ossicles in Cyprinidae. *Proc. R. Soc. Lond. B* **97**, 545-576.

Fay, R. R. (1969). Auditory sensitivity of the goldfish within the near acoustic field. *US Naval Submarine Medical Center, Submarine Base, Groton, Connecticut, Report No.* **605**, *1 11*.

Fay, R. R. (1994). Perception of temporal acoustic patterns by the goldfish (*Carassius auratus*). *Hear. Res.* **76**, 158-172.

Fay, R. R. (1998a). Auditory stream segregation in goldfish (*Carassius auratus*). *Hear. Res.* **120**, 69-76.

Fay, R. R. (1998b). Perception of two-tone complexes by the goldfish (*Carassius auratus*). *Hear. Res.* **120**, 17-24.

Fay, R. R. (2000). Spectral contrasts underlying auditory stream segregation in goldfish (*Carassius auratus*). *J. Ass. Res. Otolaryngol.* **1**, 120-128.

Fay, R. R. and Popper, A. N. (1974). Acoustic stimulation of the ear of the goldfish (*Carassius auratus*). *J. Exp. Biol.* **61**, 243-260.

Fay, R. R. and Popper, A. N. (1975). Modes of stimulation of the teleost ear. *J. Exp. Biol.* **62**, 379-387.

Fay, R. R. and Ream, T. J. (1986). Acoustic response and tuning in saccular nerve fibers of the goldfish (*Carassius auratus*). *J. Acoust. Soc. Am.* **79**, 1883.

Finneran, J. J. and Hastings, M. C. (2000). A mathematical analysis of the peripheral auditory system mechanics in the goldfish (*Carassius auratus*). *J. Acoust. Soc. Am.* **108**, 1308.

Goldberg, J. M. and Brown, P. B. (1969). Response of binaural neurons of dog superior olivary complex to dichotic tonal stimuli: some physiological mechanisms of sound localization. *J. Neurophysiol.* **32**, 613-636.

Harris, G. G. and van Bergeijk, W. A. (1962). Evidence that the lateral line organ responds to near field displacements of sound sources in water. *J. Acoust. Soc. Am.* **34**, 1831.

Hoekstra, D. and Janssen, J. (1985). Non-visual feeding behavior of the mottled sculpin, *Cottus bairdi*, in Lake Michigan. *Envir. Biol. Fish.* **12**, 111-117.

Kalmijn, A. J. (1988). Hydrodynamic and acoustic field detection. In *Sensory Biology of Aquatic Animals* (ed. J. Atema, R. R. Fay, A. N. Popper and W. N. Tavolga), pp. 83-130. New York: Springer-Verlag.

Kalmijn, A. J. (1989). Functional evolution of lateral line and inner-ear sensory systems. In *The Mechanosensory Lateral Line: Neurobiology and Evolution* (ed. S. Coombs, P. Görner and H. Münz), pp. 187-215. New York, Berlin: Springer-Verlag.

Ladich, F. and Wysocki, L. E. (2003). How does tripus extirpation affect auditory sensitivity in goldfish? *Hear. Res.* **182**, 119-129.

Morse, P. M. (1948). *Vibration and Sound*. New York: McGraw Hill.

Myrberg, A. A. and Spires, J. Y. (1980). Hearing in damselfishes: an analysis of signal detection among closely related species. *J. Comp. Physiol. A* **140**, 135-144.

Nauroth, I. E. and Mogdans, J. (2009). Goldfish and oscars have comparable responsiveness to dipole stimuli. *Naturwissenschaften* **96**, 1401-1409.

Platt, C. (1977). Hair cell distribution and orientation in goldfish otolith organs. *J. Comp. Neurol.* **172**, 283-298.

Popper, A. N. and Coombs, S. (1982). The morphology and evolution of the ear in Actinopterygian fishes. *Am. Zool.* **22**, 311-328.

Rogers, P. H. and Cox, M. (1988). Underwater sound as a biological stimulus. In *Sensory Biology of Aquatic Animal*s (ed. J. Atema, R. R. Fay, A. N. Popper and W. N. Tavolga), pp. 131-149. New York: Springer.

Sand, O. (1981). The lateral line and sound reception. In *Hearing and Sound Communication in Fishes*, pp. 459-480. New York: Springer-Verlag.

Schuijf, A. and Buwalda, R. J. A. (1975). On the mechanism of directional hearing in the cod (*Gadus morhua* L.). *J. Comp. Physiol.* **98**, 333-344.

von Frisch, K. (1938). The sense of hearing in fish. *Nature* **141**, 8-11.

Yan, H. Y., Fine, M. L., Horn, N. S. and Colon, W. E. (2000). Variability in the role of the gasbladder in fish audition. *J. Comp. Physiol. A* **186**, 435-445.

Yang, Y., Chen, J., Engel, J., Pandya, S., Chen, N., Tucker, C., Coombs, S., Jones, D. L. and Liu, C. (2006). Distant touch hydrodynamic imaging with an artificial lateral line. *Proc. Natl. Acad. Sci. USA* **103**, 18891-18895.